

Introduction to microelectromechanical systems

Warner Venstra

Kavli Institute of Nanoscience Delft
Molecular Electronics and Devices
Delft University of Technology



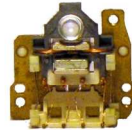
Summerschool 'Energy harvesting at micro- and nanoscales'
Workshop 'Energy harvesting: models and applications'
Erice (IT), July 23-27 2012.

I. introduction

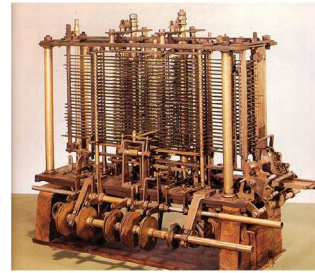
II. fabrication and characterization

III. damping and amplification of motion

electromechanical systems



CD optical pickup
Philips, 1990's



'Analytical engine'
C. Babbage, 1834



transistor computer, 1954

In the past century, transistors replaced mechanics.
At the nanoscale, mechanics can be favorable:
low dissipation, high sensitivity, new functionality.



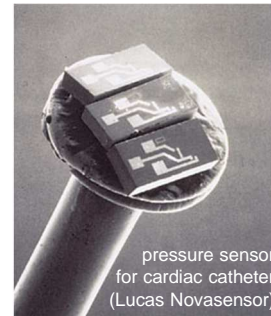
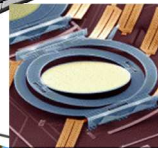
MEMS devices



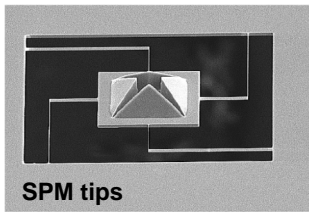
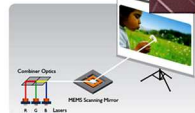
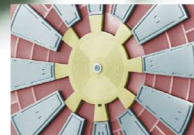
accelerometers



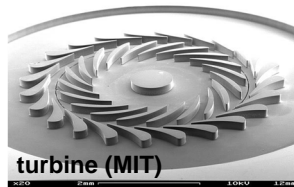
displays,
mirrors



pressure sensor
for cardiac catheter
(Lucas Novasensor)



SPM tips



turbine (MIT)



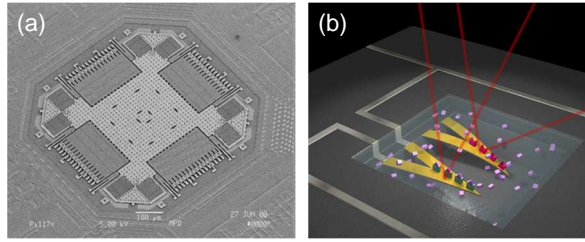
Sandia National Laboratories

MEMS in many commercial applications; turnover > 1 billion euro (big industry)



why build small mechanical systems ?

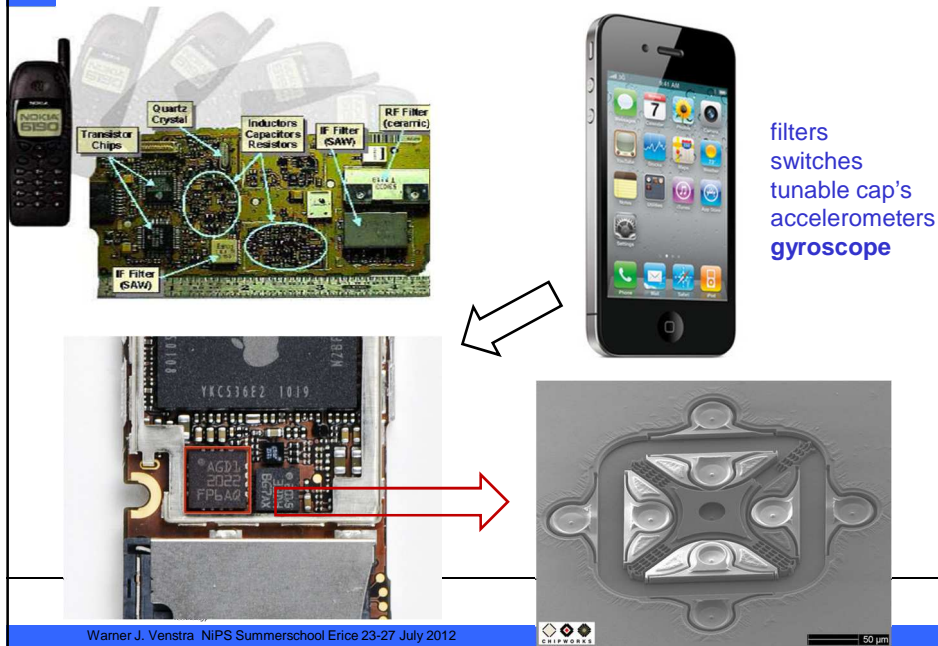
- main driver: scaling of the **surface-to-volume ratio**
- high sensitivity due to extremely low mass
- small size, batch fabrication (cheap in high volumes)
- integration with CMOS electronics: 'smart sensors'
- energy efficiency (low damping, low-dissipation switches)
- instrumentation (AFM: a mechanical lense)
- exploring new physics (quantum mechanics of large objects)
- ..



Commercial accelerometer
(Analog Devices)

Microcantilevers for sensing in liquids¹.

phones contain mechanical parts



top-down and bottom-up fabrication

top-down

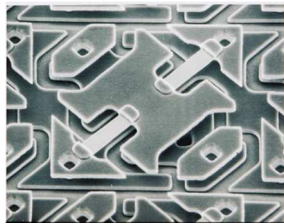
1. film deposition
2. patterning
3. etching

many layers, complex structures,
commercial, CMOS-integration,
repeatable (batch fabrication)

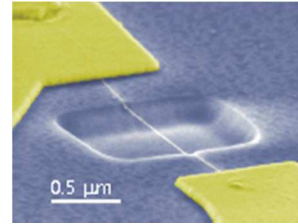
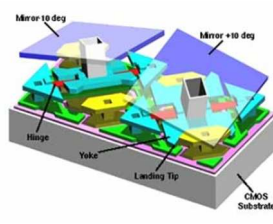
bottom-up

1. synthesis
2. (self-) alignment
3. interface

simple, ultra-small/clean structures
one-of-a-kind to study physics
poor control over dimensions

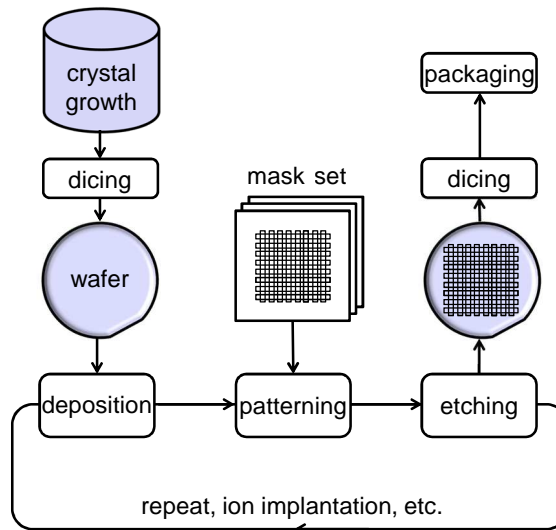


Texas Instruments Digital Mirror Device (pitch 15 μm)



suspended carbon nanotube

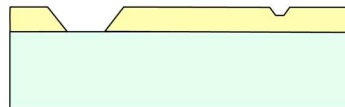
Integrated Circuit fabrication



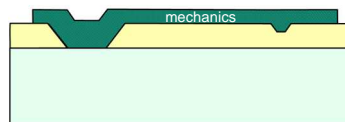
top-down fabrication: surface micromachining



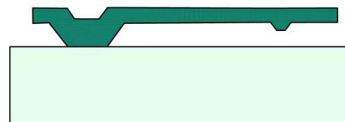
deposit a *sacrificial layer* (yellow)



define anchor points by patterning the sacrificial layer

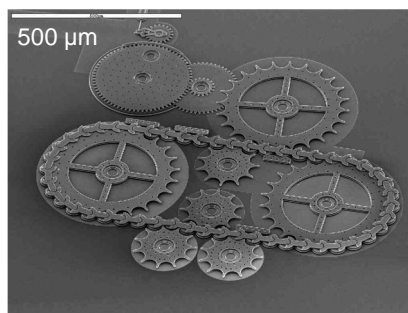


deposit *structural layer* (green) and pattern it

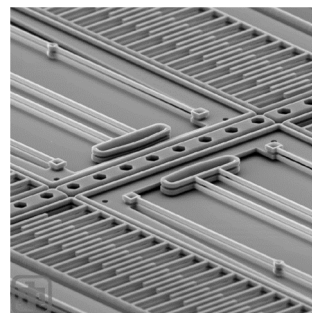


remove the sacrificial layer

surface micromachined devices

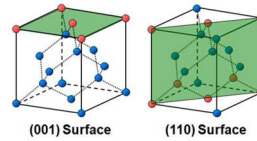


Gear system fabricated at Sandia National Laboratories: residual stress, stiction and excessive wear limit the applications of these machines.

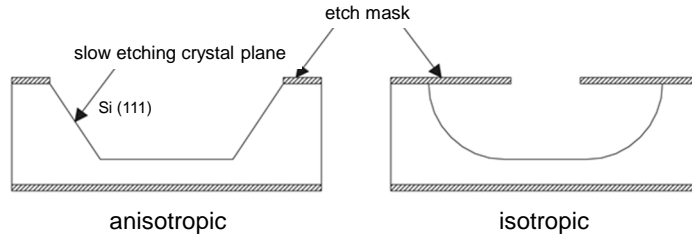


Interdigitated comb structure for electrostatic drive and motion detection (Sandia)

bulk micromachining: etching the silicon crystal



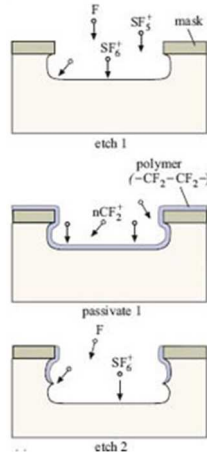
anisotropic and isotropic etching of silicon



- release of mechanical structures by 'underetching'
- create silicon proof-masses (seismic sensors, energy harvesting)
- create channels and fluid reservoirs (lab-on-chip, cooling)
- fabricate the mechanics from silicon (crystalline, high-Q)

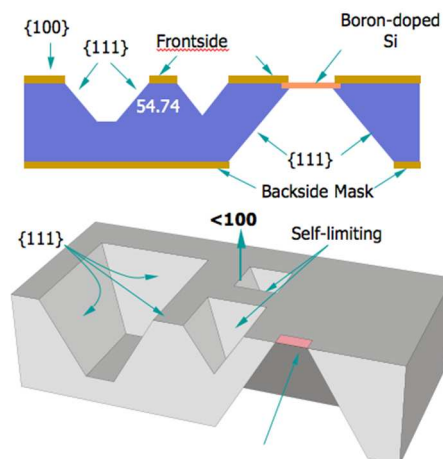
dry and wet etching of silicon

Deep Reactive Ion Etching (DRIE)



etching-passivation cycles
make process directional

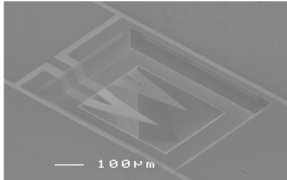
anisotropic wet etching of the Si crystal



selectivity w.r.t. crystal lattice planes

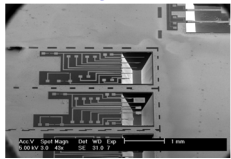
e x a m p l e s

biosensor in fluid reservoir




Venstra et al., *Microelectron. Eng.* 2012

releasing cantilevers



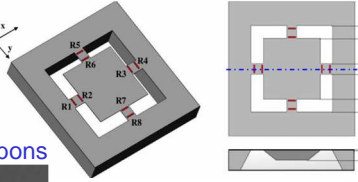
Kazinczi et al., 2007

high-Q toroid resonator



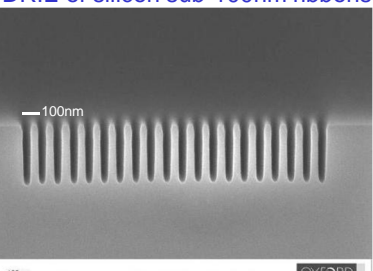
Kippenberg et al., *Science* 2010

proof-mass for an inclinometer



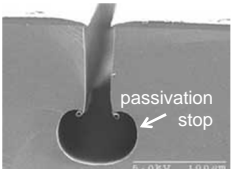
Dalola et al., *Meas. Sci. Techn.* 2012

DRIE of silicon sub-100nm ribbons



100nm
100mm WD = 5 mm EHT = 5.00 kV Signal A = InLens OXFORD

fluid channel (DRIE)



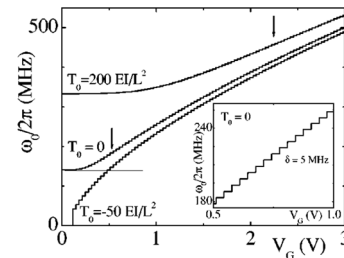
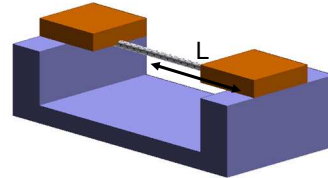
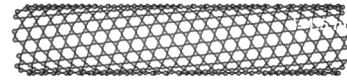
passivation stop
5.00 kV 1.00 μm

D. Gaugel et al., *Proc. IMECE 02*

top-down and bottom-up fabricated devices

bottom up: NEMS with a carbon nanotube

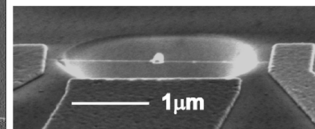
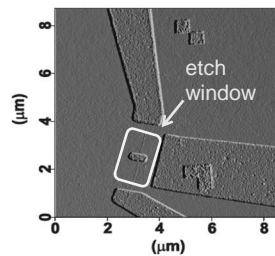
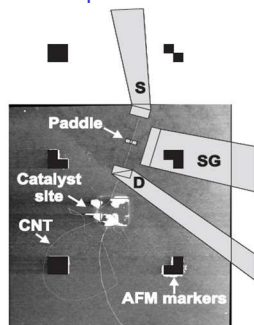
- extraordinary Young's modulus: ~ 1.2 TPa
- very low bending rigidity ($d = 2$ nm)
- smooth on atomic level: high-Q
- large thermal / zero-point fluctuations:
- route to quantum nanomechanics
- mass sensing at unprecedented resolution
- tunable over a wide range (gate)
- defect-free



S. Sapmaz et al. PRB 67 (2003)

fabrication of carbon nanotube NEMS

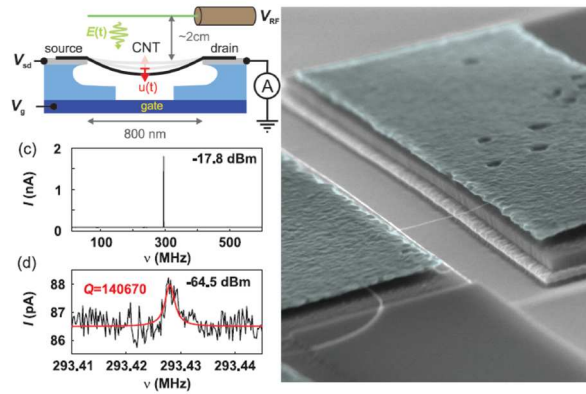
1. pattern alignment markers on a silicon wafer
2. apply catalyst (Al nanoparticles) on predefined positions
3. grow the tubes from gas phase in an oven at 900 °C
4. locate the CNT's and make the electrodes to contact them
5. suspend the CNT's (HF etching of SiO₂ and critical point drying)¹



Torsional resonator from a SW CNT³

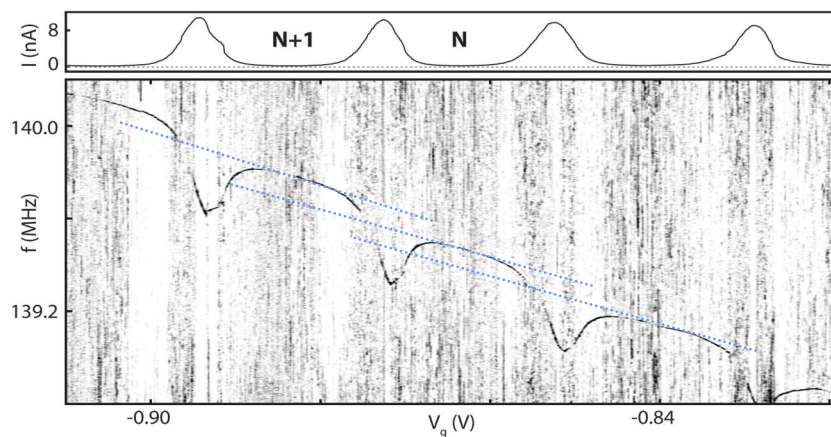
to create the etch windows, the tubes are in contact with e-beam resist. 'Dirty' Q-factors² < 100.
clean tubes can be fabricated by growing CNT's in the final step³: Clean Q can be ~ 100.000 .

example:
high-Q carbon nanotube resonators



A.K. Hüttel et al., Nano Lett.(2009)

example:
strong coupling between charge and motion



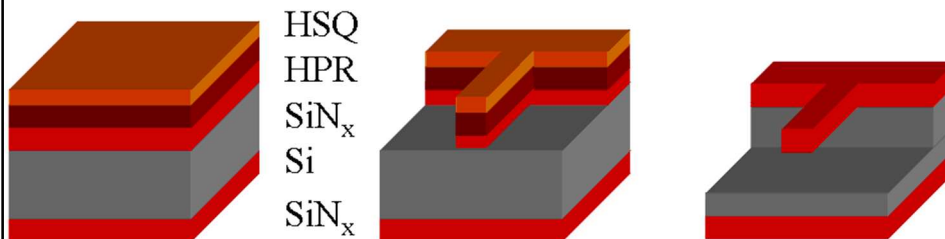
the tube is a suspended quantum dot
mechanical resonance frequency changes due to electrons tunneling on and off the dot.

G.A. Steele et al., Science(2009)

bottom-up fabrication is a 'mix':
tubes grow in random direction
the electrodes are fabricated top-down

top-down fabrication: silicon nitride resonators

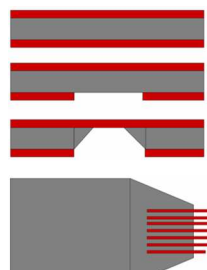
LPCVD SiN is an excellent, homogeneous material, with low pinhole density
residual stress is relatively low: $\sim 60 \text{ MPa}$ ¹
suitable as an etch mask for Si, but also to fabricate mechanics



two resist layers: HSQ for e-beam and HPR as a protective mask²

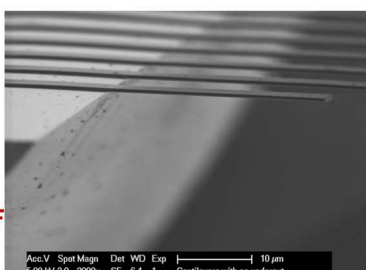
releasing the structures

anisotropic wet etching through a window on the backside: **no undercut**

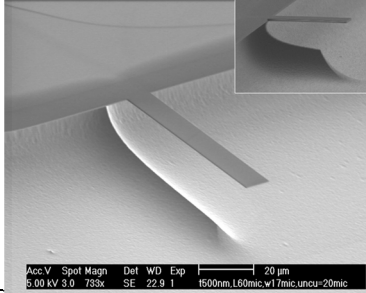


undercut increases the effective length¹. Mechanical properties of the SiN depend on the release process².

¹ K. Babaei Gavan et al., JMM 035003 (2009)
² K. Babaei Gavan et al., Microelectron. Eng. 86 (2009)




Acc.V Spot Magn Det WD Exp 5.00 kV 3.0 2000x SE 6.4 1 10 μm
Cantilevers with no undercut



Acc.V Spot Magn Det WD Exp 5.00 kV 3.0 783x SE 22.9 1 20 μm
1500nm,160mic,w17mic,uncut-20mic

isotropic wet or dry etching: **undercut**

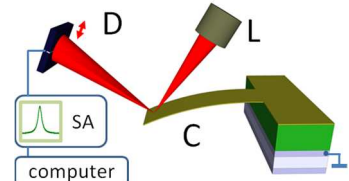


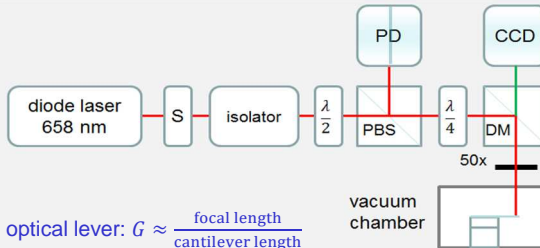
Delft University of Technology

Warner J. Venstra NiPS Summerschool Erice 23-27 July 2012

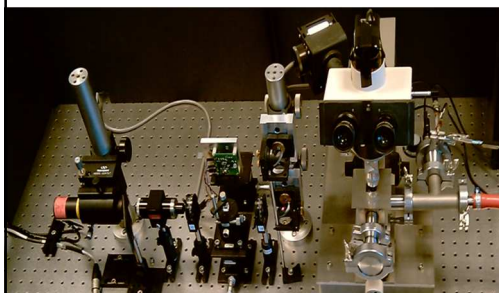
21

characterization by optical deflection technique






optical lever: $G \approx \frac{\text{focal length}}{\text{cantilever length}}$



sensitivity $\sim 1\text{pm}/\sqrt{\text{Hz}}$
 thermal noise measurements
 at room temperature in
 vacuum, air and **liquids**

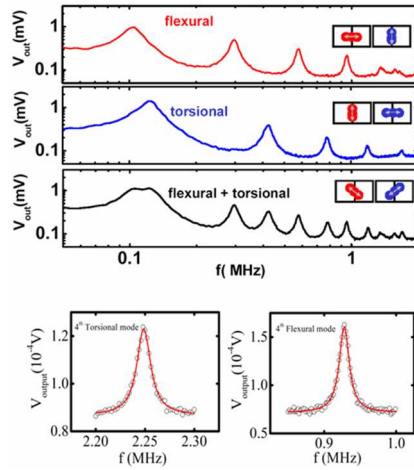


Delft University of Technology

Warner J. Venstra NiPS Summerschool Erice 23-27 July 2012

22

thermal noise spectrum: flexural and torsional modes



Euler-Bernoulli beam theory:

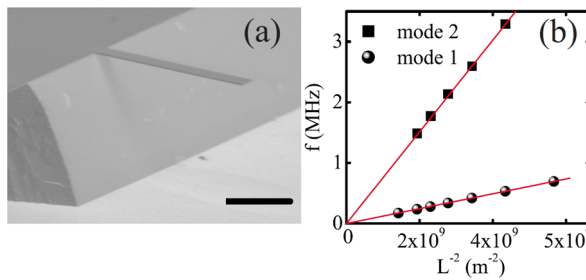
$$\text{flexural modes: } f_n = \frac{\alpha_n^2}{2\pi\sqrt{12}} \frac{t}{L^2} \sqrt{\frac{E}{\rho}}$$

$$\text{torsional modes: } f_n = \frac{2n-1}{4L} \sqrt{\frac{\eta G}{\rho I_p}}$$

$$\text{equipartition: } \langle x_n^2 \rangle = \frac{k_B T}{m(f_n/2\pi)^2}$$

cantilever dimensions $L \times w \times t = 60 \times 17 \times 0.074 \mu\text{m}^3$

determination of Young's modulus



The Young's modulus E_{eff} is determined by measuring the length-dependence of the resonance frequency for the lowest two modes, and fitting them to the Euler Bernoulli beam equation:

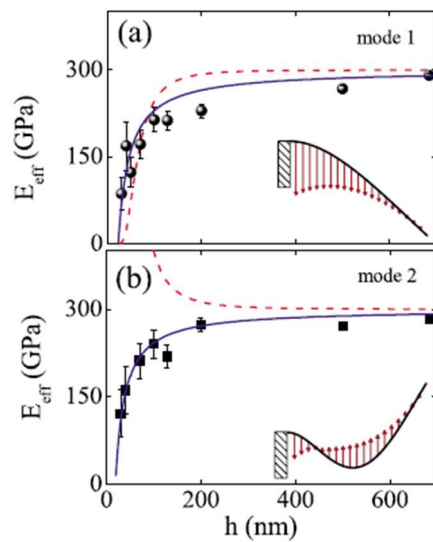
$$f_n = \frac{\alpha_n^2}{2\pi\sqrt{12}} \frac{t}{L^2} \sqrt{\frac{E_{eff}}{\rho}}$$

with $\alpha_{1,2} = 1.875, 4.694$.

In thin devices, the surface free-energy¹ should give rise to a decrease in the observed Young's modulus

¹energy to create a surface out of the bulk, in liquids known as surface tension

E_{eff} sharply drops for thin (<150nm) structures !

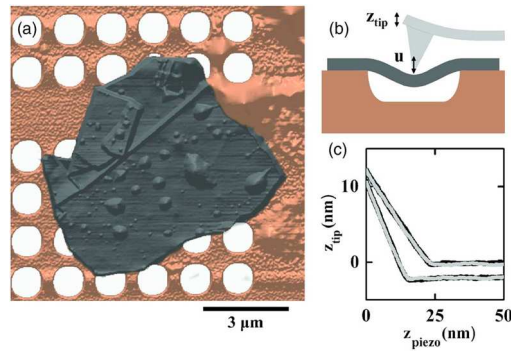


size-dependent material properties were observed in silicon before. Is it related to the surface tension?

data for the second mode rules out the strain-independent surface stress model (red).

a surface elasticity model (blue) fits the data for the two modes consistently¹.

surface tension studies require thinner and more homogeneous structures: few-layer graphene?



mechanics of few-layer graphene: M. Poot et al. APL 92 063111 (2008)

small dimensions → large tolerances

poorly defined mechanics¹ due to:

- undercut
- process-dependent material props
- inhomogeneity across the thickness of deposited layers
- surface elasticity
- residual stress gradients
- bad definition of clamps (cnt's, Si beams)
- creep and relaxation ('burn-in')
- geometric effects due to pattern transfer
- ...

tolerance (relative uncertainty in the dimensions) increases upon scaling down

but: easy tuning since small systems are compliant and couple strongly

on-chip calibration in applications such as resonant sensors, mirror devices, air-bag sensors etc.

imperfections break the symmetry, and become important when designing mechanical systems with low energy barriers such as switches

a route towards well-defined micromechanics

Silicon wafers are typically diced along the (100) surface;
when diced along (110), the (111) sidewalls are vertical.

high aspect-ratio, well-defined geometry and clamps, low surface roughness

IOP PUBLISHING

JOURNAL OF MICROMECHANICS AND MICROENGINEERING

J. Micromech. Microeng. 21 (2011) 075011 (5pp)

doi:10.1088/0960-1317/21/7/075011

Fabrication of tunable clamped-clamped microresonators in silicon (110)

R van Leeuwen, P H R Lew, E W J M van der Drift, H S J van der Zant
and W J Venstra

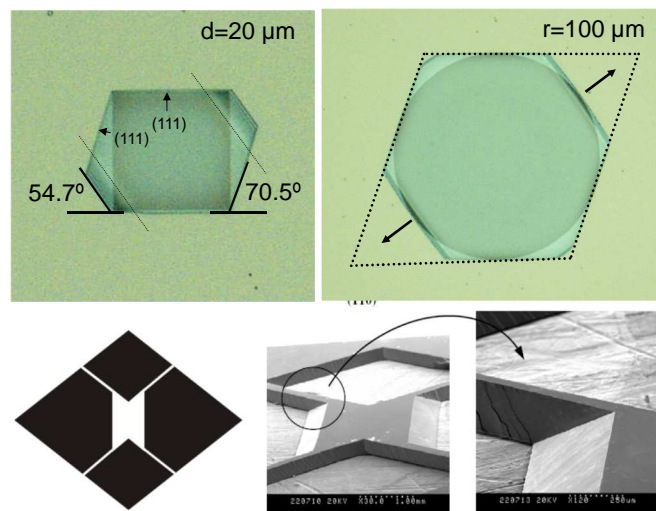
Kavli Institute of Nanoscience, Lorentzweg 1, 2628CJ Delft, The Netherlands



Warner J. Venstra NIPS Summerschool Erice 23-27 July 2012

29

anisotropic wet etching of Si(110)



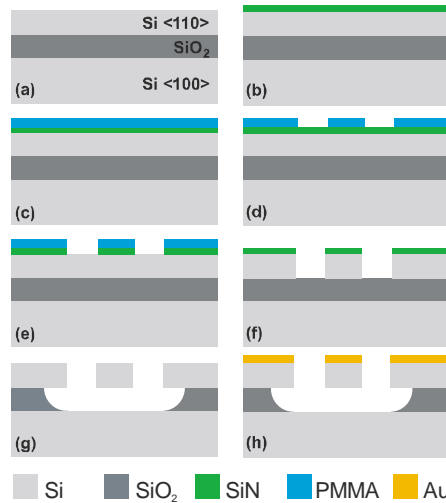
Zubel and Kramkowska, J. Micromech. Microeng. (2005)



Warner J. Venstra NIPS Summerschool Erice 23-27 July 2012

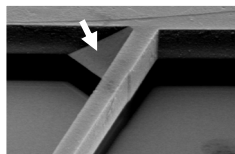
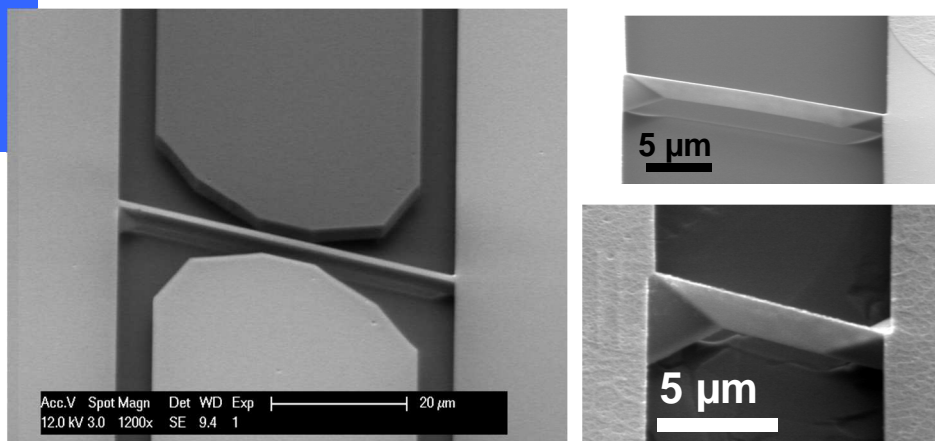
30

fabrication of mechanical resonators in SOI (110)



- (a) SOI wafer, 2 μm (110) device layer
 (b) PECVD of 30 nm SiN hard mask
 (c) spin coating of 50 nm PMMA
 (d) E-beam patterning
 (e) RIE of SiN (CHF₃/Ar)
 (f) KOH etching of Si
 (g) BHF etching of SiO₂
 (h) evaporation of 100 nm Cr/Au layer

results



- single exposure process
- resonators with thickness <100nm (CPD required)
- convex corners constrain side gates
- different clamp geometry: etching stops at (111) planes spanned across the corners

characterization

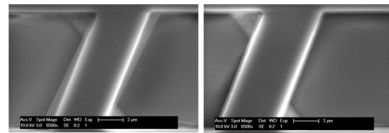
composite beam: $f_n = \frac{\alpha_n^2}{2\pi L^2} \sqrt{\frac{\sum_i E_i I_i}{\sum_i \rho_i A_i}}$

- i : layer index
- E_i : Young's modulus
- I_i : moment of inertia ($I = \frac{wt^3}{12}$)
- ρ_i : mass density
- A_i : cross section area

For $L \times w \times t = 150 \times 1.6 \times 2 \mu\text{m}^3$, the calculated frequencies are:
 $f_1=500 \text{ kHz}$; $f_3=2.70 \text{ MHz}$. The measured ones are $f_1=513 \text{ kHz}$; $f_3=2.76 \text{ MHz}$.

- clamped-clamped resonators in SOI (110): stress-free crystals, smooth sidewalls
- critical geometry is determined by slowly etching (111) planes
- gate-tuning over a few percent

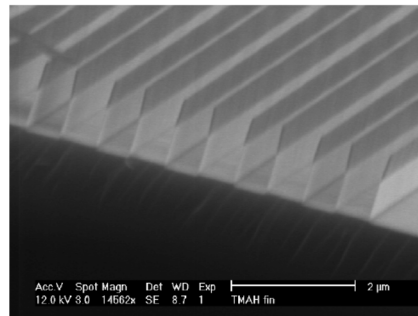
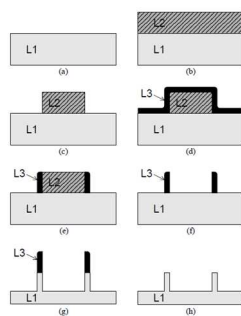
accuracy frequency of the devices matches the calculation within 5 %



critical parameter: alignment between mask and crystal lattice

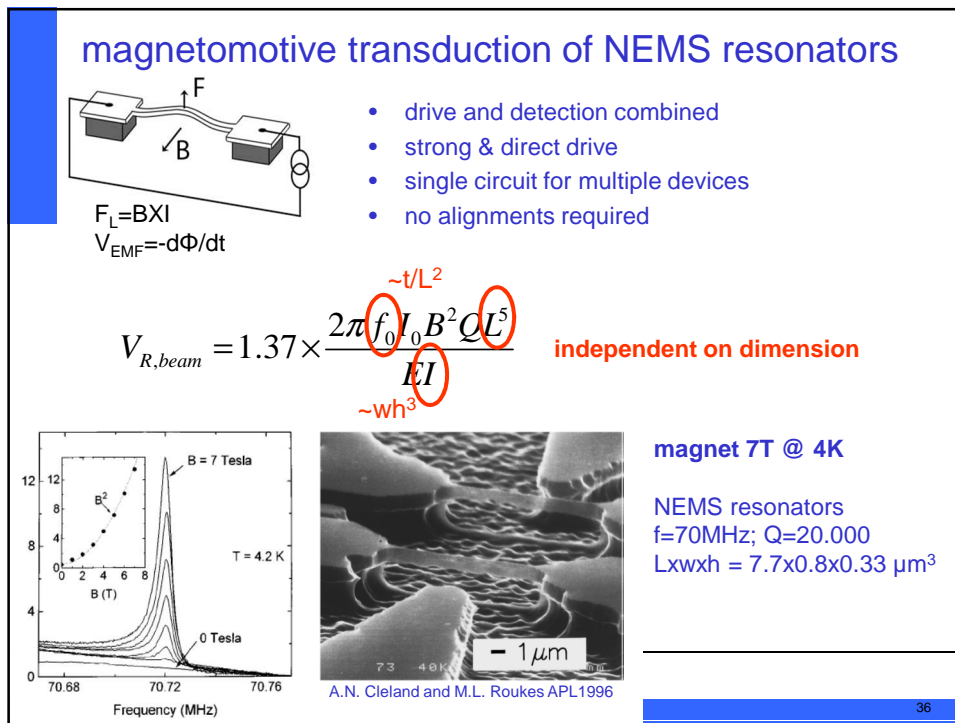
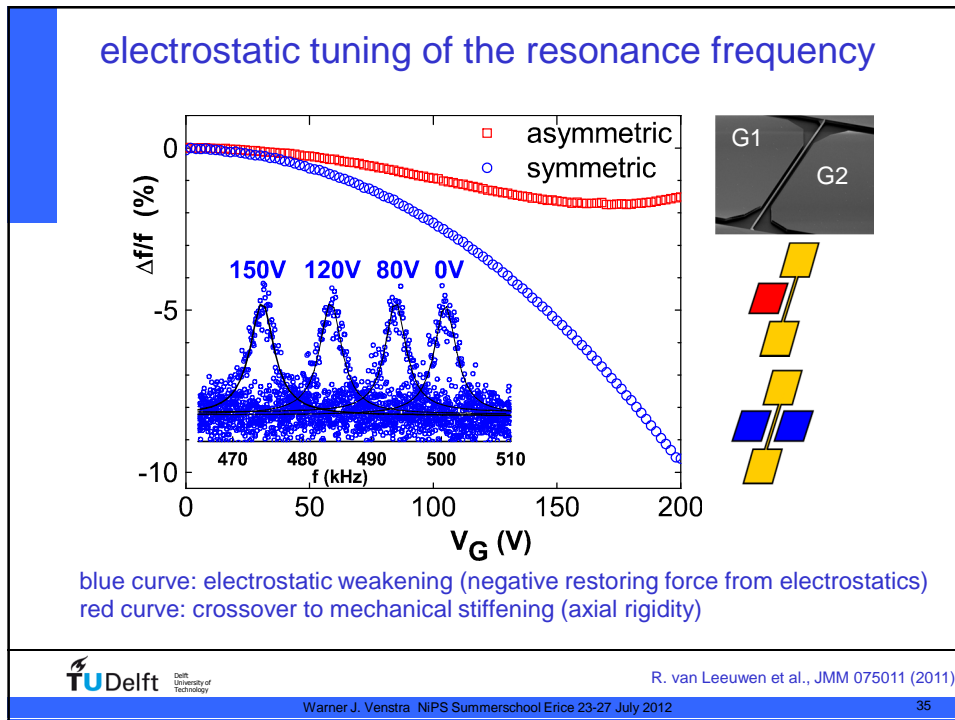
self-aligned mask

define the mask on a (111) sidewall (cf. 10nm Fin-FET's)



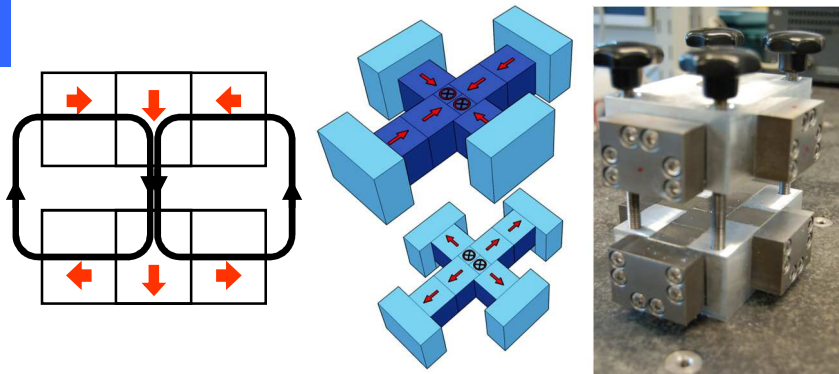
V. Jovanović et al., 2002

a 'suspended fin' resonator
 challenge: definition of clamping points



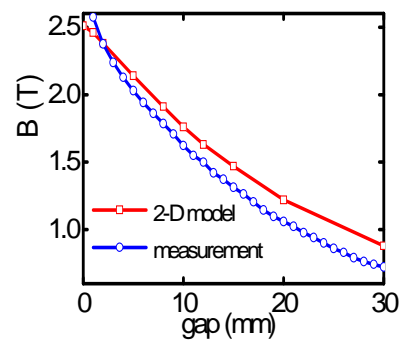
room temperature: Halbach magnet

strong field in a large gap



1 inch³ NdFeB magnets ($B_r=1.5$ T) magnet size: 12 x 15 x 9 cm³

$B > 2$ T at room temperature



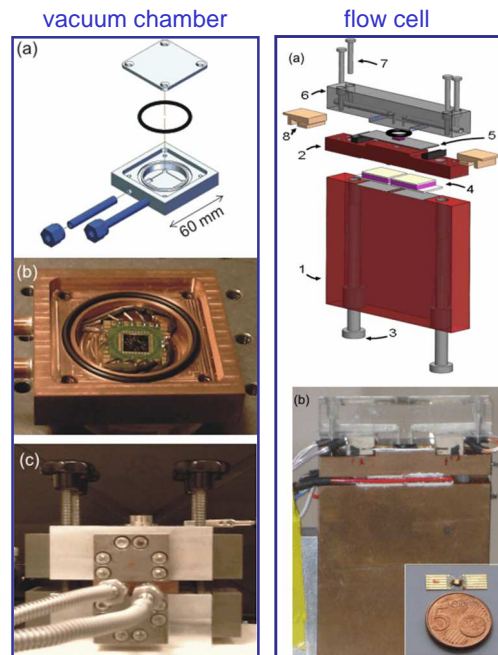
$B > 2.5$ T in 1 mm gap

$B \sim 2$ T in 6 mm gap: insert vacuum chamber or liquid cell
homogeneous field in a 6 x 6 x 6 mm³ volume:

- sample alignment is not critical
- simultaneous measurement of multiple devices

motion detection in vacuum air liquids

- thermal noise in vacuum
- in water: strong driving
- nonlinear behavior
- readout of resonator arrays



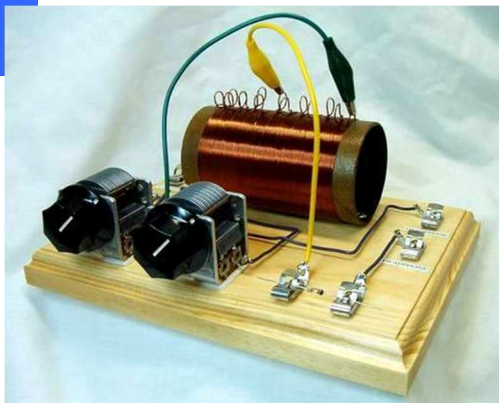
summary

- fabrication technologies: top-down and bottom-up
- unique property: large surface-to-volume ratio
- small-scale mechanics: large tolerances
- detection methods:
 - electrostatic mixing (CNT's)*
 - optical deflection*
 - magnetomotive*
 - on-chip piezoelectric transducers*
 - capacitive*
- growing number of applications
 - instrumentation*
 - signal processing*

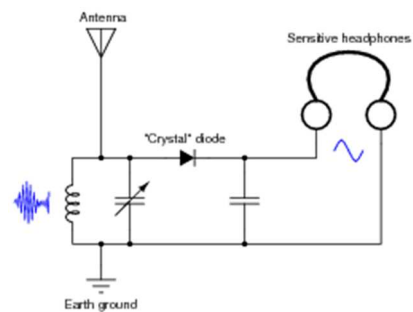
damping and amplification of motion in micromechanical resonators

- I. damping mechanisms in mechanical resonators
 - dissipation to environment
 - internal damping
- II. modification of the damping in mechanical resonators
 - parametric excitation
 - external feedback
- III. damping and amplification via coupled modes

energy harvesting anno 1900



electromagnetic energy harvesting

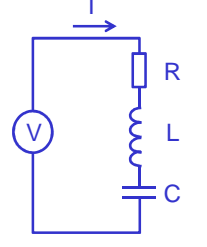


Zeropower:

AM radiowaves power the earphone

damping in resonant systems

electrics

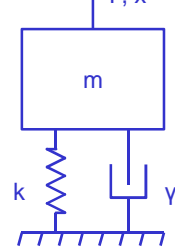


RLC-circuit

$$\ddot{I} + \frac{R}{L}\dot{I} + \frac{1}{LC}I = 0$$

$$Q_E = \frac{1}{R}\sqrt{\frac{L}{C}} < 1000$$

mechanics

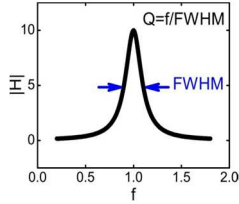


mass-spring-damper

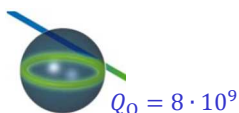
$$\ddot{m}x + \underbrace{\frac{m\omega_0}{\gamma}}_Y \dot{x} + \underbrace{m\omega_0^2}_k x = 0$$

$$Q_M = 1 \cdot 10^7$$


Q-factor measures the capability to store energy:

$$Q = \frac{\text{stored energy}}{\text{rate of energy loss}}$$


optical systems



$$Q_0 = 8 \cdot 10^9$$



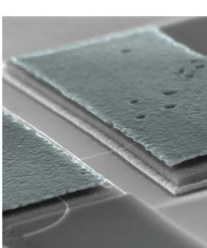
Delft University of Technology

Vahala Nature 2003

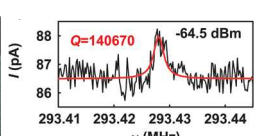
Warner J. Venstra NIPS Summerschool Erice 23-27 July 2012


43

high-Q mechanics




carbon nanotube resonator
 $Q=10^5$ $f \cdot Q = 10^{13}$
 Hüttel et al., Nano Lett. 2009



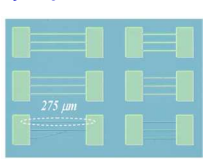


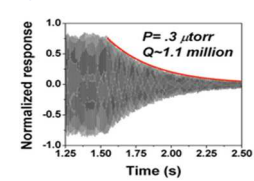
tuning fork: $Q=1000$
 $f \cdot Q = 440.000$

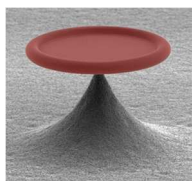


Virgo mirror suspension spring: $Q=10^7$
 $f \cdot Q = 10^{10}$
 Travasso et al., Europhys Lett. 2007


top-down SiN tensile strings: $Q=10^6$
 $f \cdot Q = 10^{12}$ Verbridge et al., APL 2008







toroid resonator
 $Q=10^8$
 $f \cdot Q = 10^{14}$
 Kippenberg Science 2010



Delft University of Technology

Warner J. Venstra NIPS Summerschool Erice 23-27 July 2012

44

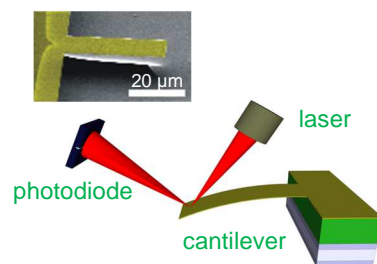
damping mechanisms

<i>external:</i>	viscous drag molecular collisions clamping losses adsorption/desorption ...	} $\frac{1}{Q_{\text{total}}} = \sum_i \frac{1}{Q_i}$
<i>internal:</i>	thermoelastic damping surface effects two-level systems modal interactions ...	

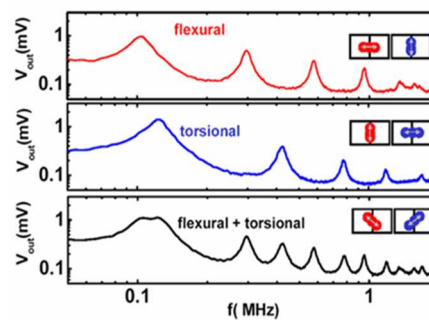
Q-factor is phenomenological: regime determines dominant damping mechanism

carbon nanotube resonator in Coulomb blockade: charge noise
high-tension silicon nitride string : clamping losses

external damping: the environment dominates



'optical lever' as in AFM



Brownian motion at atmospheric pressure: bending and torsion modes

$$\text{equipartition: } \langle x^2 \rangle = \frac{k_B T}{k_R}$$

measure the dynamics of a mechanical resonator in different environments

resonators in liquids: low Q

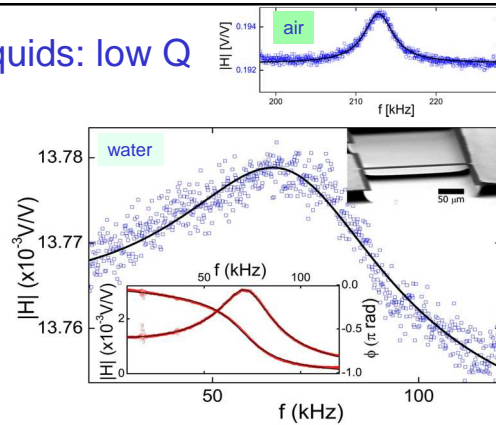
mechanical Q
 vacuum: 10^3 - 10^7
 ambient: 10-500
water: <10

- huge drop in f: mass loading
- Q increases w. mode number
- complex drag force can be modeled

hydrodynamic function $\Gamma(\text{Re}, \kappa)$ relates cross-section to inertial and viscous force:

$$r_n = \frac{f_{n,\text{water}}}{f_{n,\text{vac}}} = \left[1 + \frac{\pi W \rho}{4t \rho_c} \Gamma_R(\text{Re}, \kappa) \right]^{-0.5}$$

E.O. Tuck, J. Eng. Math. 3 (1969) 1
 Van Eysden and Sader, Phys. Fluids (2006);

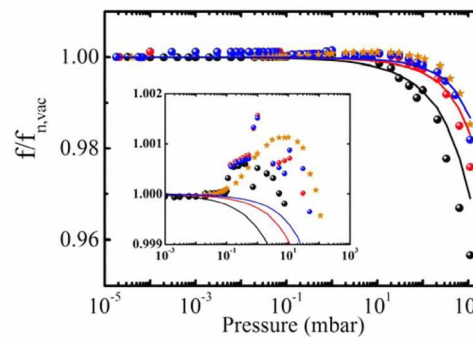
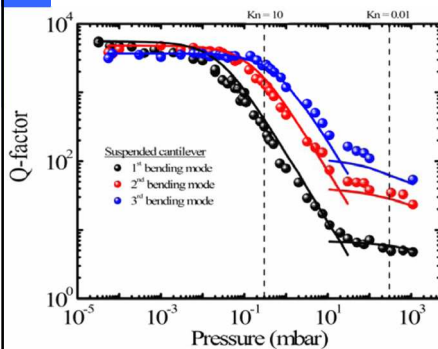


n	frequency (kHz)				Q-factor		
	air	water	f_{theory}	f_{exp}	air	water	$water_{\text{theory}}$
1	194.9	52.6	0.23	0.27	50	2.0	4.1
3	593.3	184	0.25	0.31	67	5.4	6.7

Venstra and Van der Zant, APL 95 (2009) 263103



in gas there are 3 regimes



3 regimes: viscous fluid damping, molecular regime, intrinsic damping

strongly reduced mass loading: f_0 decreases by a few %

inset shows anomalous rise in frequency from $P=10^{-1}..10^2$ mbar with $f/f_{\text{vac}} > 1$



K. Babaei Gavan et al., Proc. IEEE NEMS (2009)

molecular regime

momentum exchange between individual gas molecules at a rate proportional to the difference in velocity between mechanics and the molecules:

$$Q_{mol} = \left(\frac{\pi}{2}\right)^{3/2} \frac{\sqrt{R_0 T / M_m}}{P} t \rho_c f_n$$

squeeze-film damping plays a significant role, and can be modeled.

Knudsen number: $Kn = \frac{\lambda}{w}$

for a device with $w = 2 \text{ nm}$; at atmospheric pressure $\lambda \sim 6 \cdot 10^{-8} \text{ m}$ yields $Kn = 30$
carbon nanotubes could be in the intrinsic regime at atmospheric pressure !

TU Delft Delft University of Technology
 Warner J. Venstra NIPS Summerschool Erice 23-27 July 2012 49

the fundamental limit to *intrinsic* damping ?

The community actively debates on the ultimate limit to the Q-factor in mechanical resonators.

- thermoelastic damping (Zener)
- clamping losses
- two-level systems
- surface reconstruction
- modal interactions

Wang et al., JMEMS 2000

Unterreithmeier et al., PRL 2010

Colet et al., Nat Comm 2011

Warner J. Venstra NIPS Summerschool Erice 23-27 July 2012 50

MODIFYING THE DAMPING

parametric amplification ($f_{\text{drive}} \neq f_{\text{res}}$)



Instead of periodically varying the force, vary ('pump') a system parameter, for example the spring constant:

$$m\ddot{x} + \frac{m\omega_R}{Q}\dot{x} + [m\omega_R^2 + \underbrace{k_p \sin(2\Omega t + \varphi)}_{\text{parametric excitation}}]x + \alpha x^3 = \underbrace{F \cos(\Omega t)}_{\text{direct excitation}}$$

this can be used for

- amplification of the vibration without broadening of the response (Q_{eff} enhances)
- beyond threshold: self-sustained oscillation (amplitude limited by nonlinearities)

technologically of great interest:

pre-amplification in the mechanical domain for detectors of force, mass etc.

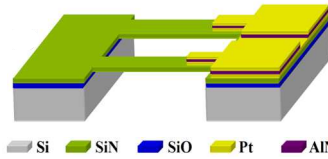
First demo in a microresonator by Rugar and Grütter (PRL 67(6)1991):

VOLUME 67, NUMBER 6

PHYSICAL REVIEW LETTERS

5 AUGUST 1991

parametric amplification in piezo-resonators



$$m\ddot{x} + \frac{m\omega_R}{Q}\dot{x} + [m\omega_R^2 + \overset{\text{parametric excitation}}{k_p \sin(2\Omega t + \varphi)}]x + \alpha x^3 = \overset{\text{direct excitation}}{F \cos(\Omega t)}$$

- voltage on piezo modulates the spring constant by changing the stress in the beam

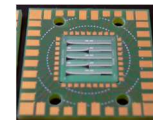
- gain on resonance: $G(\varphi) = \sqrt{\frac{\cos^2(\varphi + \pi/4)}{(1 + k_p/k_t)^2} + \frac{\sin^2(\varphi + \pi/4)}{(1 - k_p/k_t)^2}}$

- instability at $k_p = k_t$

- non-Lorentzian response: $A = \frac{F_0 Q}{m\omega_0^2} \cdot \frac{2Q(\omega_D - \omega_R) - i\omega_R}{\omega_0(\omega_D - \omega_R)^2 + 4iQ(\omega_D - \omega_R) + \omega_R(1 - \frac{k_p}{k_t})}$

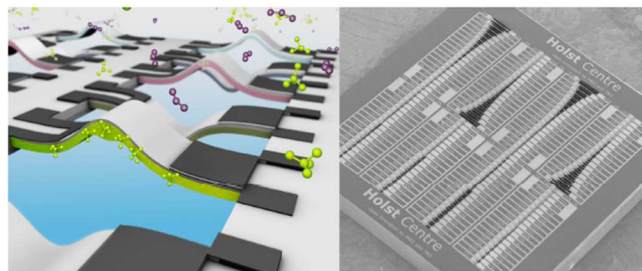


resonators with on-chip piezo transducer



Enhanced Volatile Detection with Low Power Integrated Micromechanical Resonators

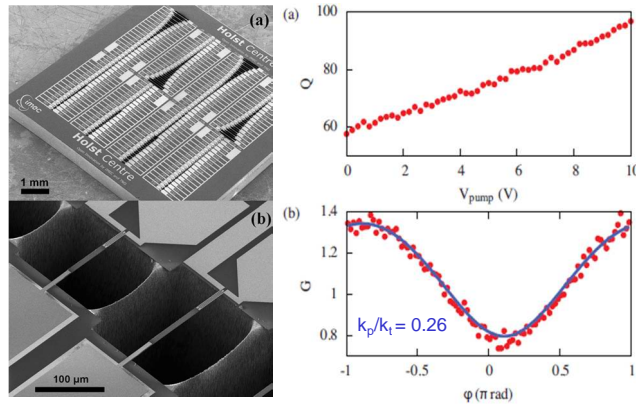
D. M. Karabacak, S. Brongersma and M. Crego-Calama



Polymer coated, very high aspect ratio doubly-clamped beam resonators with integrated transducers are demonstrated for ultra-low power, high sensitivity detection of volatile compounds.

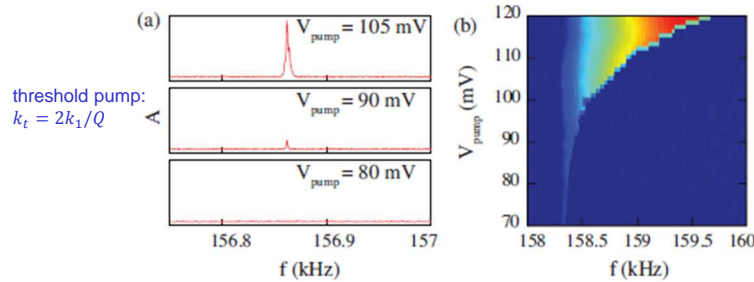


parametric amplification and attenuation of motion

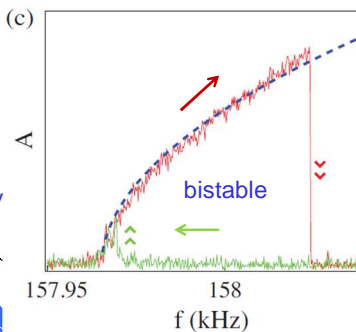


Q-enhancement of weakly driven system, $f_{drive}=2f_0$ at $\phi=3\pi/4$
 depending on ϕ the motion is amplified or attenuated

parametric instability: $k_p > k_t$ results in oscillations



- the amplitude of the parametric oscillation, A , is proportional to the square root of the pump frequency: $|A| \sim \sqrt{f_{pump}}$ (dotted line)
- nonlinear behaviour:
 1. amplitude explodes beyond threshold
 2. amplitude-dependent resonance frequency
 3. bistable phase

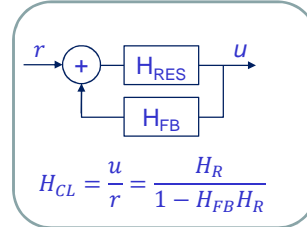


feedback

transfer functions:

$$\text{resonator: } H_{RES} = \frac{1/k}{1 - \left(\frac{\omega}{\omega_0}\right)^2 + \frac{i\omega}{Q\omega_0}}$$

$$\text{feedback: } H_{FB} = Ge^{i\varphi}$$



$$\text{closed-loop: } H_{CL} = \frac{H_{RES}}{1 - H_{FB}H_{RES}} = \frac{\frac{1}{k} \left(1 - \frac{\omega^2}{\omega_0^2} - \frac{G}{k} \cos \varphi \right) - \frac{i}{k} \left(\frac{\omega}{Q\omega_0} - \frac{G}{k} \sin \varphi \right)}{\left(1 - \frac{\omega^2}{\omega_0^2} - \frac{G}{k} \cos \varphi \right)^2 + \left(\frac{\omega}{Q\omega_0} - \frac{G}{k} \sin \varphi \right)^2}$$

stiffness damping

feedback: special cases

velocity-proportional feedback when $\varphi = \frac{2n-1}{2}\pi$ $n = 1, 2, \dots$

the damping is modified: $\frac{1}{Q_{eff}} = \frac{1}{Q} - \frac{G}{k}$

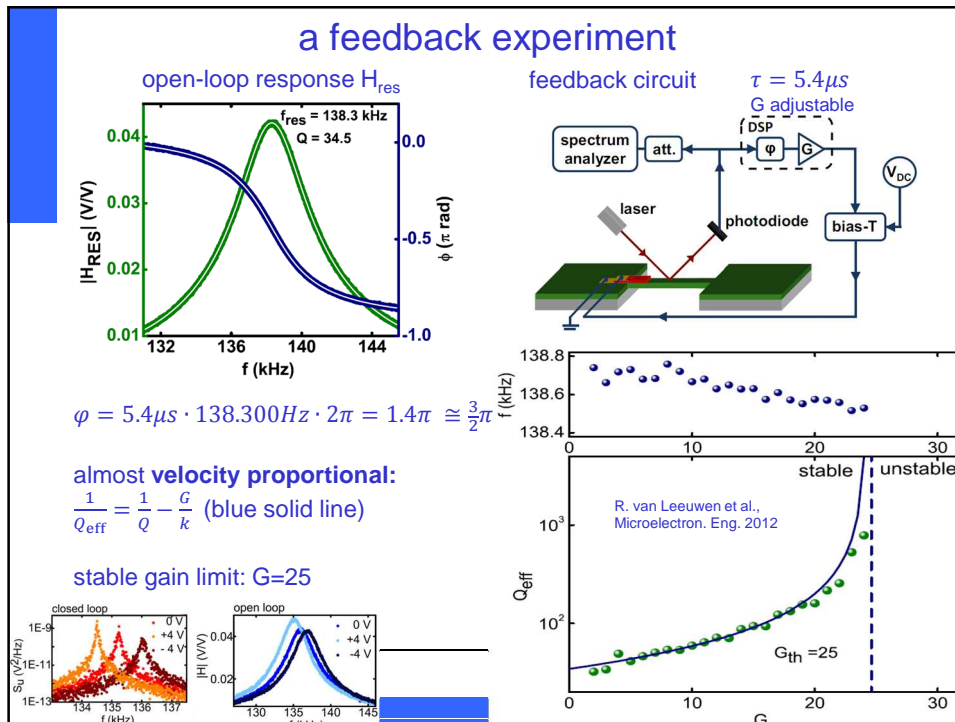
displacement-proportional feedback ($\varphi = n\pi$) the spring constant is modified

limited stability

gain on resonance: $|H_{CL}| = \left((G \cos \varphi)^2 + \left(\frac{k}{Q} - G \sin \varphi \right)^2 \right)^{-\frac{1}{2}}$

$\varphi = \frac{\pi}{2}, G = \frac{k}{Q}$ (or equivalently: $\varphi = \frac{3\pi}{2}, G = -\frac{k}{Q}$): 'Barkhausen criterion'

in practice φ is the result of a delay time in the system



damping and amplification of motion
via
modal interactions

nonlinearity couples the vibration modes

Delft University of Technology

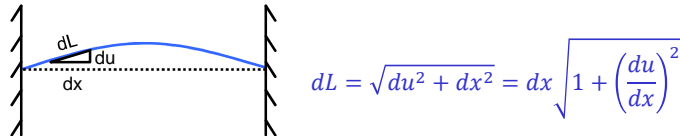
Warner J. Venstra NIPS Summerschool Erice 23-27 July 2012

60

extensional: fixed on two sides (bridges, membranes)



origin of nonlinearity: displacement-induced tension



Elongation against the axial rigidity EA/L results in a tension T:

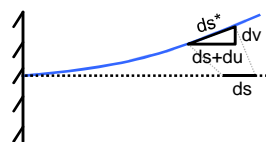
$$T = \frac{EA}{2L} \int_0^L \left(\frac{du}{dx}\right)^2 dx$$

E: Young's modulus
A: cross section

inextensional: displacements without extending (cantilever)



origin of nonlinearity: inextensionality condition



$$\text{strain: } \epsilon = \frac{ds^* - ds}{ds} = \frac{\sqrt{(ds+du)^2 + dv^2}}{ds} - 1$$

$$\text{inextensionality: } \epsilon = 0$$

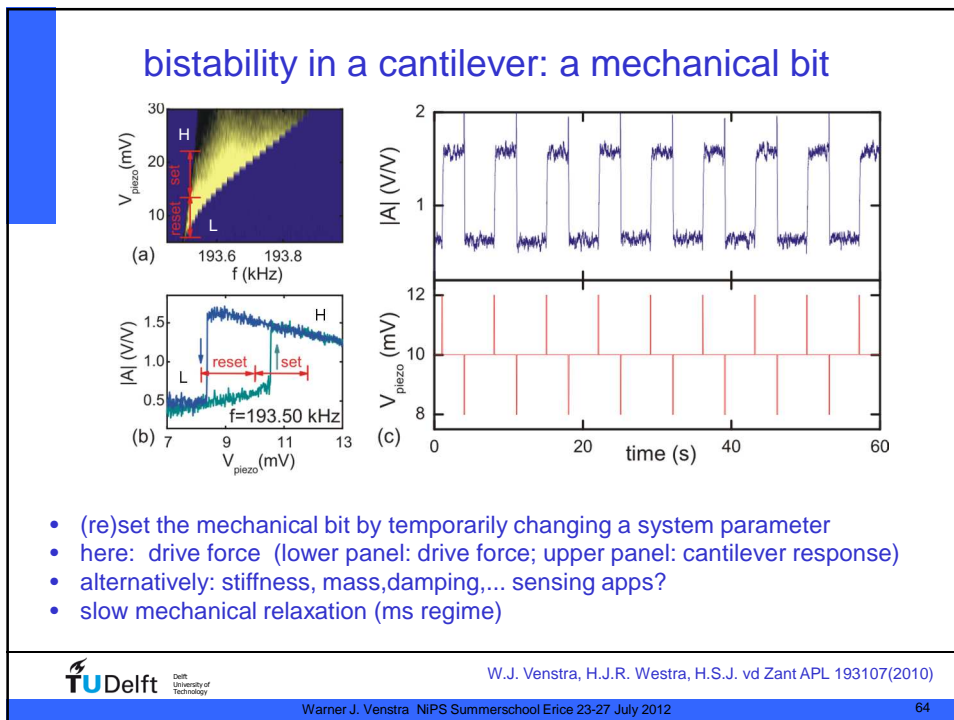
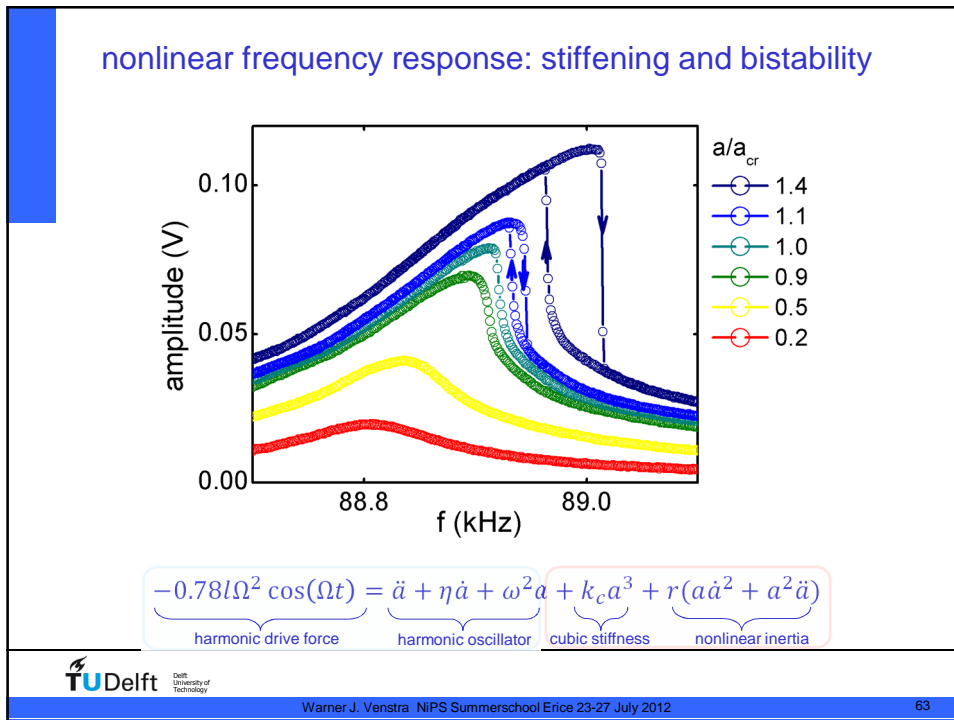
$$\text{coupling: } (1 + u')^2 + v'^2 = 1$$

no extension of the neutral axis

geometry couples horizontal and vertical displacements for all modes

horizontal displacement (u) couples the flexural modes

flexure couples also to torsion

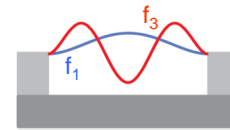
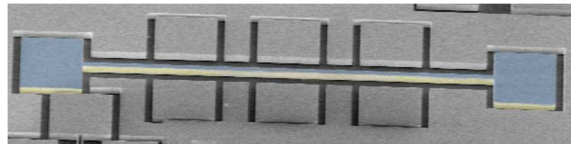


Nonlinear Modal Interactions in Clamped-Clamped Mechanical Resonators

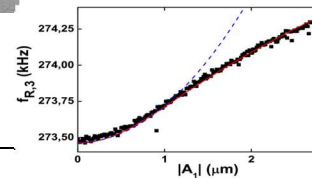
H. J. R. Westra,* M. Poot, H. S. J. van der Zant, and W. J. Venstra

Kavli Institute of Nanoscience, Delft University of Technology, Lorentzweg 1, 2628CJ Delft, The Netherlands
(Received 6 April 2010; revised manuscript received 6 July 2010; published 10 September 2010)

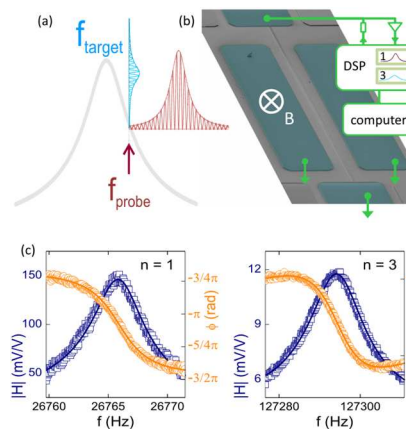
A theoretical and experimental investigation is presented on the intermodal coupling between the flexural vibration modes of a single clamped-clamped beam. Nonlinear coupling allows an arbitrary flexural mode to be used as a self-detector for the amplitude of another mode, presenting a method to measure the energy stored in a specific resonance mode. The observed complex nonlinear dynamics are quantitatively captured by a model based on coupling of the modes via the beam extension; the same mechanism is responsible for the well-known Duffing nonlinearity in clamped-clamped beams.



Duffing nonlinearity: tension induced by a displacement changes the resonance frequency of all the modes: $f_i \propto |a_j|^2$

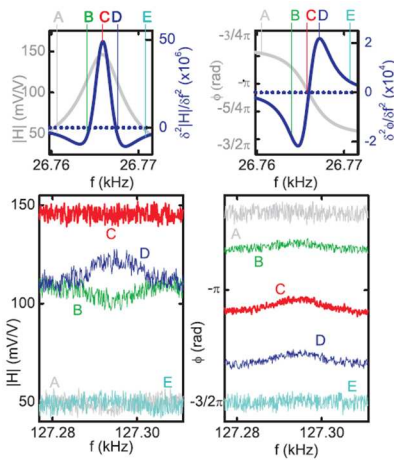


weak driving, strong tuning



- no signatures of a nonlinearity in the individual freq. responses
- weakly driven 3rd mode modulates the motion of the fundamental mode
- tool: swept-frequency response measurements of higher modes

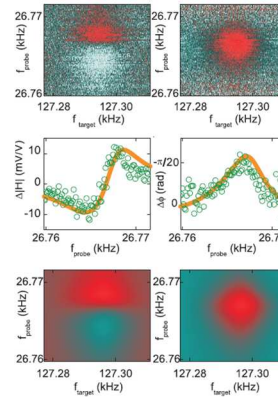
coupled 3rd mode modulates the response of the 1st mode



modal interactions can be modeled by displacement-induced tension. It is *dispersive* coupling. Dissipative?

drive strength ~1000 k_BT

linewidth 5.8Hz ↔ tuning 0.8 Hz



coupling strength: 0.09Hz/nm²
limits Q<450.000 @ RT

nonlinear interactions between flexural modes

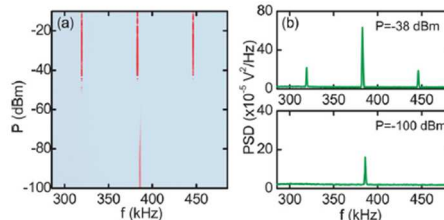
eq. of motion including the coupling

$$\ddot{u}_i + \eta_i \dot{u}_i + \omega_i^2 u_i + \sum_{j=1}^n \sum_{k=1}^n \sum_{l=1}^n \left(\alpha_{ijkl} u_j u_k u_l + \frac{1}{2} \beta_{ijkl} u_j (u_k u_l) \right) = f_i \cos(\Omega_i t)$$

again, the coupling coefficients are the integrated modeshapes

$$\alpha_{ijkl} = \int_0^1 \xi_i \{ \xi_j' (\xi_k' \xi_l'') \}' ds,$$

$$\beta_{ijkl} = \int_0^1 \xi_i (\xi_j' \int_1^s \int_0^{s_2} \xi_k' \xi_l' ds_1 ds_2)' ds.$$

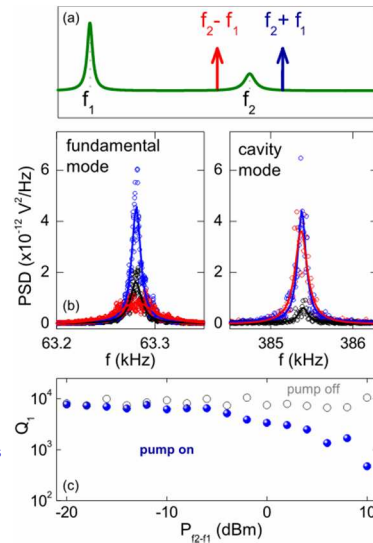


evidence of coupling: motional sidebands at mixing frequencies of mode 1 and 2

coupled modes: phonon-phonon cavities

- a mechanical equivalent of cavity optomechanics
- geometric nonlinearity couples modes
- modification of the Q-factor
- damping and amplification of the thermal noise peak
- prospects:
 - cooling?
 - interactions between the flexural and torsional modes; degeneracy

W.J. Venstra, H.J.R. Westra, H.S.J. van der Zant. Q-factor control of a microcantilever by mechanical sideband excitation APL 99 (2011) 151904.



I. Mahboob, K. Nishiguchi, H. Okamoto, H. Yamaguchi, Phonon cavity electromechanics Nat Phys 8 (2012) 387

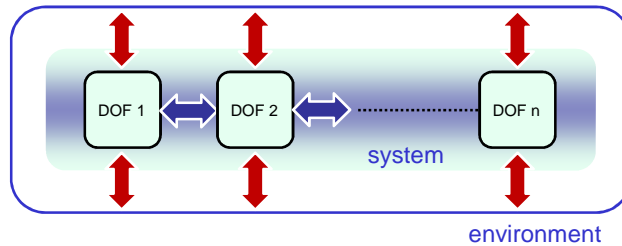
Phonon-cavity electromechanics

Mahboob, K. Nishiguchi, H. Okamoto & H. Yamaguchi
Affiliations | Contributions | Corresponding authors
Nature Physics (2012) | doi:10.1038/nphys2277
Received: 07 November 2011 | Accepted: 23 February 2012 | Published online: 01 April 2012 | Corrected online: 26 April 2012

Warner J. Venstra NIPS Summerschool Erice 23-27 July 2012

69

damping summary



- ↔ dispersive coupling (no change in energy of system)
 - thermoelastic damping
 - reconstruction of material
 - two-level systems
 - modal interactions
 - ↕ dissipative coupling (system leaks to environment)
 - viscous drag
 - molecular collisions
 - clamping losses
 - adsorption/desorption
- harvesting transducer**



Warner J. Venstra NIPS Summerschool Erice 23-27 July 2012

70

Thank You

contact:
Warner Venstra
Faculty of Applied Sciences
Kavli Institute of NanoScience
Delft University of Technology
Lorentzweg 1, 2628 CJ Delft
The Netherlands
w.j.venstra@tudelft.nl

